[1*]Aroob Alhassani
[1]Layan Baabdullah
[1]Rana Almehmadi
[1]Anfal Hathah
[1]Sultan Alghamdi

Designing a Z-Source Microinverter for Low-Input Voltage Solar Applications

Journal of Electrical Systems

Abstract: - The global transition to renewable energy emphasizes the role of photovoltaic systems, where inverters are essential. This paper investigates microinverters tailored for individual solar panels, recognizing the need to customize the outputs of each panel due to their inherent low voltage of solar cells. Size reduction and efficiency enhancement are also among the goals of microinverters. Significant progress in boosting capabilities and enabling integration with grid and home applications highlights the promising potential of Z-source microinverters in photovoltaic systems. Notably, achieving a substantial boosting factor of nearly four suggests significant potential for further optimization, complemented with a total harmonic distortion of less than 5%, indicating improved efficiency and compatibility with existing infrastructure. This research presents the integration of the Z Source topology into microinverter design as a promising solution to address the challenge of low voltage output from individual solar panels for residential use, contributing to the global transition towards sustainable energy solutions. To evaluate the advantages of employing Z source inverters, this paper uses the Simulink simulation tool to analyze associated design aspects and control mechanisms.

Keywords: Microinverter, Photovoltaic system, Renewable energy, Total harmonic distortion, Z-source impedance.

I. INTRODUCTION

The global community has recognized the critical importance of renewable energy sources in addressing the challenges of climate change and sustainable development, with a notable emphasis observed in Saudi Arabia through highlighted projects [1-2]. Solar energy, in particular, has garnered significant attention and widespread adoption due to its ease of installation and abundant availability. In the process of harnessing electricity from solar energy, inverters play a crucial role by converting the Direct Current (DC) power generated by solar panels into Alternating Current (AC) power compatible with most applications and the grid [3].

Inverters utilized in Photovoltaic (PV) systems are classified into three main types based on their size and application into microinverters, string inverters, and central inverters [4]. Each type is tailored for specific purposes, with central inverters designed for high-power applications, while microinverters are suitable for low-wattage levels and residential use.

Traditionally, microinverters have been deployed using a two-stage approach involving a DC converter followed by either Voltage Source Inverters (VSI) or Current Source Inverters (CSI) [5]. However, these conventional methodologies present inherent limitations and introduce additional losses to the system.

To overcome these limitations, the Z Source Inverter (ZSI) topology has emerged as a viable alternative solution [6]. The ZSI incorporates a distinctive impedance network comprising inductors and capacitors arranged in a crossed Z-shaped configuration. This arrangement allows the ZSI to address the drawbacks of both VSI and CSI systems without requiring a separate DC stage [7]. Moreover, the intentional use of the shoot-through state in the ZSI aids in achieving voltage boosting, thereby enhancing its overall performance while reducing Total Harmonic Distortion (THD).

This paper integrates a microinverter with ZSI design to enhance efficiency and reduce size in single-panel installations for residential use. The paper is structured as follows: Section II gives a PV inverter overview; Section III covers topology and component analysis. Section IV discusses control techniques for the microinverter, followed by simulations in Section V. Section VI concludes with future outlook.

[1] Department of Electrical and Computer Engineering, Faculty of Engineering, King Abdulaziz University, Jeddah 21589, Saudi Arabia.
*Corresponding author: Aroob Alhassani, Email: Aroob.Alhassani@gmail.com.

II. INVERTERS IN PHOTOVOLTAIC SYSTEMS

The selection of suitable PV inverter is paramount for optimizing performance and cost-effectiveness in solar installations. As shown in [8], the inverters used in PV systems can be categorized into centralized, microinverter, and string configurations., each tailored to specific deployment scenarios and operational needs. Microinverter PV systems emerge as highly effective solutions for residential and small-scale commercial applications due to their ability to maximize energy production from each panel. This makes microinverters particularly suitable for residential rooftops and distributed generation setups. In contrast, centralized PV systems are strategically utilized in large-scale solar projects, emphasizing cost efficiency and simplified maintenance for utility-scale solar farms and commercial ventures. String PV systems occupy a niche in medium-scale solar projects, such as commercial buildings and small solar farms, offering a balance between cost-effectiveness and performance.

In the following sections, the emphasis will be on microinverters because they are well-suited for addressing low-input voltage scenarios commonly encountered in residential settings.

III. TOPOLOGIES OF MICROINVERTERS

Exploring microinverter development involves evaluating different configurations, including two-stage microinverters and one-stage microinverters with or without transformers. Nevertheless, striking a harmonious balance between efficiency, component reduction, and performance poses significant challenges. Therefore, it is imperative to design microinverters that effectively optimize these factors, reducing the size and intricacies and ensuring efficient and dependable performance. The incorporation of the Z-source topology offers a promising solution to addressing these challenges. This is exemplified in Fig.1, which illustrates a single-phase ZSI configuration connected to a PV system. The Z-source inverter configuration plays a pivotal role in effectively handling low-input voltage scenarios with just one stage. This is made possible due to the unique Z impedance before the inverter bridge, which facilitates an increase in voltage. The mechanism behind this voltage boost involves the utilization of the shoot-through state. This shoot-through state is achieved by precisely controlling the switches of the inverter bridge and establishing a direct connection between the DC source and the load without requiring an additional DC-DC boost converter.

In addition to this control, the functionality of the PV system is enhanced through the Maximum Power Point Tracking (MPPT) algorithms. Therefore, the combination of the ZSI configuration and MPPT control mechanisms ensures efficient utilization of the PV system and reliable operation even in low input voltage conditions.

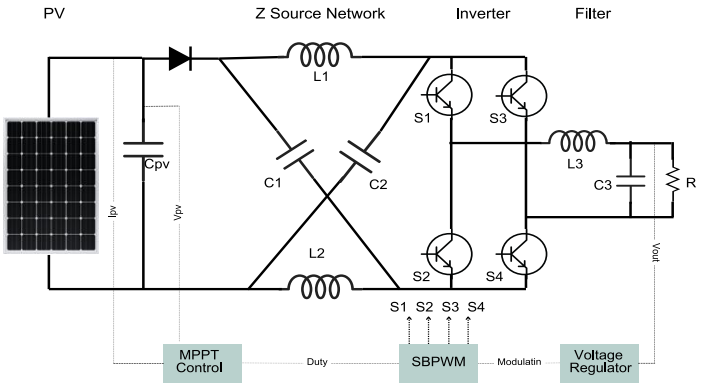

Fig. 1 Overview of the System

The switches of the inverter achieve the shoot-through state and consequently, the voltage-boosting effect. Effective control of these switches' ON and OFF states is paramount for attaining the desired output. The inverter system operates with two primary switching states: shoot-through and non-shoot-through (zero and active states), as detailed in Table 1.

During the zero states, the load terminals are shorted through either the lower or upper switches, while in the active states, the DC voltage is connected across the load. In the shoot-through state, which is intentionally introduced at specific intervals, the load terminals are simultaneously shorted through both the upper and lower switches of one or two legs. This arrangement allows current to flow directly and enhances the voltage output from the PV panel.

Table 1. States of the Switches

Switching States	S1	S2	S3	S4	Output Voltage
Active States	1	0	0	1	Finite Voltage
	0	1	1	0	
Zero States	1	0	1	0	Zero
	0	1	0	1	
Shoot Through State	1	1	S3	S4	Zero
	S1	S2	1	1	
	1	1	1	1	

A. Analysis of Z-Source Inverter

Continuing from the previous explanation, the shoot-through state, illustrated in Fig. 2, presents a distinctive configuration where the diode connected to the input side operates in the opposite direction. In Fig.1, capacitors C1 and C2 assume critical roles in this state as they are responsible for charging the inductors, L1 and L2, respectively. Notably, the voltage across the inductors equates to the voltage across the capacitors, in accordance with previous studies [9].

$$V_C=V_L \tag{1}$$

During the shoot-through interval (T0), DC link voltage across the inverter bridge is

$$V_{DC\ Link}= 0 \tag{2}$$

$$V_{PV}=2V_C=V_{C1}+V_{C2}>V_{PV} \tag{3}$$

In the non-shoot trough state, shown in Fig.3 , the currents flowing through the inductors (L1, L2) and the capacitors (C1, C2) are:

$$I_{L1}=I_{C1}= I_{L2}=I_{C2} \tag{4}$$

The diode connected at the input side is conducting, allowing current to flow through it. The voltage across the inductors:

$$V_L=V_{PV}-V_C \tag{5}$$

During the non-shoot-through, interval (T1), the dc-link voltage across the inverter bridge is:

$$V_{DC\ Link}= V_C-V_L=2V_C-V_{PV} \tag{6}$$

The total duration of the shoot-through and non-shoot-through intervals:

$$T= T_0+T_1 \tag{7}$$

In the steady state, the average voltage across $V_{L1}=0$ during the entire switching period T:

$$(V_C)\ T_0+(V_{PV}- V_C)T_1 =0 \tag{8}$$

$$\frac{V_C}{V_{PV}}= \frac{T_1}{T_1- T_0} \tag{9}$$

The average DC ink voltage can be determined by considering the periods T1, T0:

$$V_{DC\ Link}=\frac{T_0*0+ (V_{PV}- V_C)T_1}{T}=\frac{(V_{PV}- V_C)T_1}{T}=\frac{T_1}{T_1- T_0}\ V_{PV} \tag{10}$$

$$\frac{T_1}{T_1- T_0}\ V_{PV}= V_C \tag{11}$$

$$V_{DC\ Link}=V_{PV}\ B \tag{12}$$

Where B represents the boosting factor:

$$B= \frac{T_1}{T_1- T_0}=\frac{1}{1-\left(2\frac{T_0}{T}\right)}\geq 1 \tag{13}$$

Combining the equations, the peak phase voltage of the output from the inverter can be represented as:

$$V_{AC}=\frac{MV_{dcLink}}{2}=\frac{M\ B\ V_{PV}}{2} \tag{14}$$

Where M denotes the modulation index ($M \leq 1$).

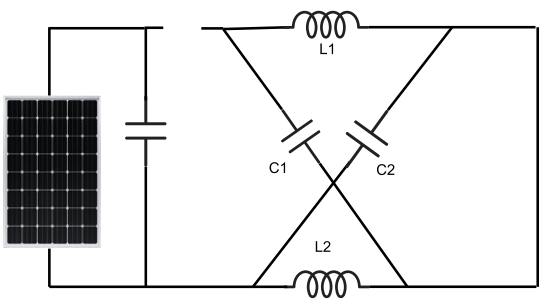

Fig. 2 Shoot-Through State

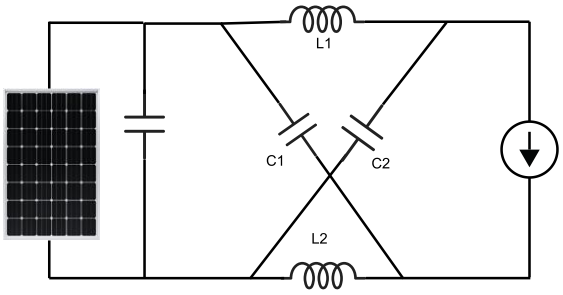

Fig. 3 Non-Shoot-Through State

B. Component Selection

The Z-source inverter configuration includes both an inductor and a capacitor, and selecting the appropriate values for these components is critical to ensure the optimal performance and stability of the inverter system. The selection process is carried out as follows:

1) Inductor Design.

During the shoot-through mode, the current flowing through the inductor increases linearly, and the voltage across the inductor is equal to the voltage across the capacitor.

During the non-shoot-through mode, the current flowing through the inductor decreases linearly, and the voltage across the inductor is the result of subtracting the capacitor voltage from the input voltage of the PV system.

The average current flowing through the inductor:

$$I_L = \frac{P}{V_{PV}} \tag{15}$$

The maximum current ripple through the inductors occurs when the maximum shoot-through condition is present.

Inductor Max current,

$$I_{Max} = I_L + \text{CurrentRipple\%} \tag{16}$$

Inductor Min current,

$$I_{Min} = I_L - \text{CurrentRipple\%} \tag{17}$$

During shoot-through,

$$V_L = V_C \tag{18}$$

The value of the inductor can be determined by calculations using.

$$L = \frac{V_L * T_0}{\Delta I}\ ,\ \Delta I = I_{Max} + I_{Min} \tag{19}$$

2) Capacitor Design.

The purpose of the capacitor is to absorb the fluctuations in current and maintain a relatively stable voltage to ensure the output voltage remains sinusoidal. During the shoot-through period, the capacitor charges the inductors, and the current passing through the capacitor is equal to the current flowing through the inductor.

The calculation of the capacitor value can be done by using.

$$C = \frac{(I_L * T_0)}{\Delta V}\ ,\ \Delta V = \text{VoltageRipple\%} \tag{20}$$

IV. CONTROL AND OPERATION PRINCIPLE

The implementation of the Z-topology in a microinverter requires careful attention to various control aspects. The control process involves multiple stages, starting with the MPPT algorithm on the DC side, which ensures stable output from the solar panel. The control then focuses on regulating the AC output and processing it to determine the appropriate pulse signals for each switch using one of the PWM methods, thereby achieving the desired boosting function.

A. DC Side.

The control mechanism on the DC side utilizes the Perturbation and Observation (P&O) method, a well-established technique for tracking the Maximum Power Point (MPP) in PV systems. As detailed in [10-11], this

method involves analyzing the P-V curve to pinpoint the MPP, where the output is maximized. Fig. 4 shows the P-V curve for different irradiance levels. Through perturbation, the P&O algorithm dynamically adjusts the operating point of the PV system, optimizing power production at the MPP. This iterative process guarantees that the PV system operates with utmost efficiency, thereby maximizing energy generation.

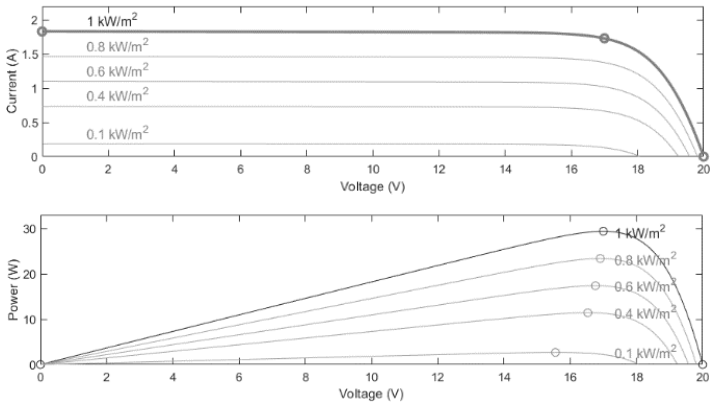

Fig. 4 (Current and Voltage) and (Power and Voltage) Curves with Variable Irradiation

B. Simple Boost Pulse Width Modulation.

The primary function of this controller is to generate Pulse Width Modulation (PWM) signals with the shoot-through configuration, thereby controlling the switches and achieving the desired output as investigated in [12]. Both the results of Simple Boost Pulse Width Modulation (SBPWM) signals and the MPPT algorithm are utilized as inputs to the switches, accurately regulating their ON and OFF states. Hence, following the calculations derived from the MPPT algorithm, two DC shoot-through lines, referred to as envelopes, are generated, indicating a relationship between the Modulation index (M) and the shoot-through duty ratio. This relationship is expressed by $D = 1 - M$. These lines are then compared with a triangular carrier waveform operating at a frequency of 10kHz to determine the shoot-through duty ratio. In the shoot-through condition, when the carrier waveform exceeds the positive and negative DC lines, all switches are turned ON, allowing for the injection of shoot-through states, which facilitates the boosting operation. Otherwise, the controller compares two sinusoidal waves with a frequency of 60Hz and a phase shift of 180 degrees with the carrier. This comparison generates the necessary conditions for a non-shoot-through state, guiding the appropriate switching patterns for the switches. The states of the switches resulting from comparing the carrier with the DC lines and the sinusoidal references are shown in Fig.5.

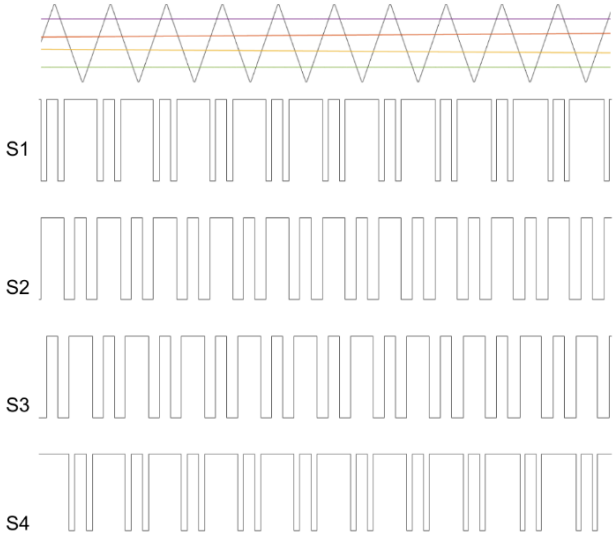

Fig. 5 Switching States with Shoot Through Intervals

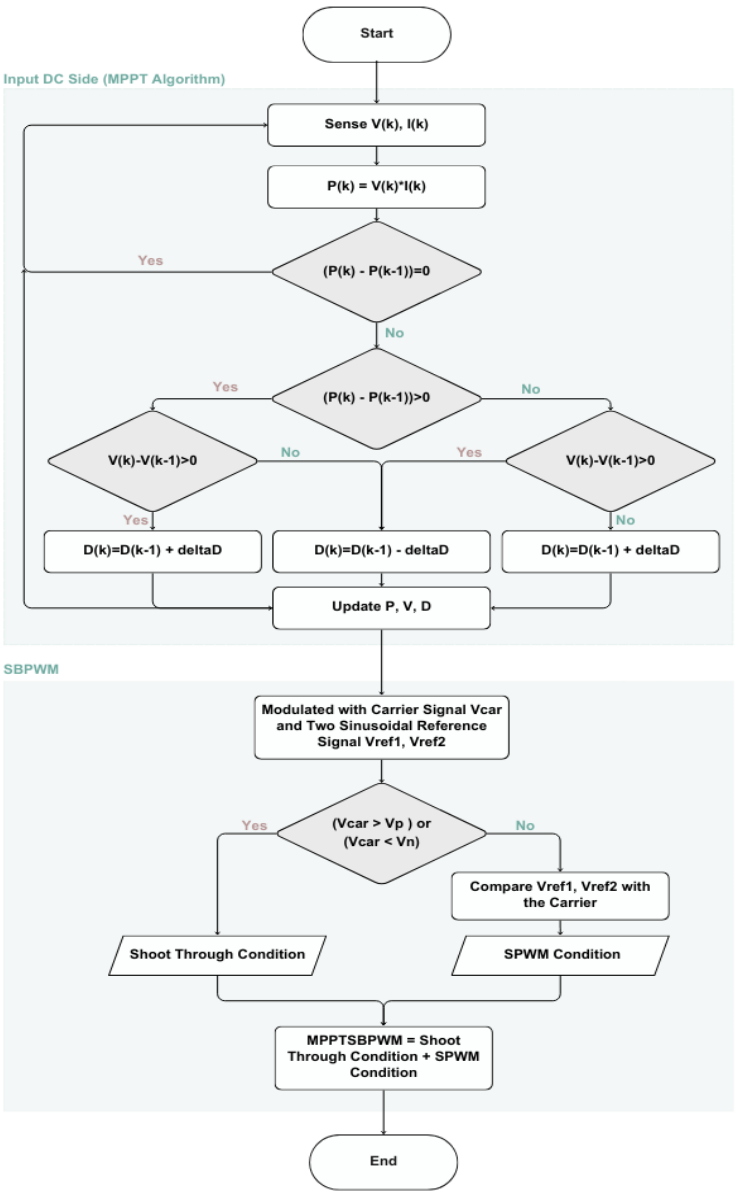

Fig. 6 Control Procedure

V. SIMULATION

The simulation is conducted to demonstrate the feasibility of increasing a small voltage level, showcasing the effectiveness of the Z-source-based microinverter as a viable option in PV residential. The specifications of the system were derived using the equations detailed in Section 3, particularly (19) and (20).

As a result, the specifications of the Z-source inverter were determined as follows: Z-impedance with inductance of 10 mH, capacitance of 47 µF, and frequency of the inverter bridge switches at 10 kHz.

The simulation was conducted using Simulink. This simulation involved the utilization of inputs from the solar system, specifically temperature and irradiance data from the photovoltaic system. The outputs of the simulation included current and voltage readings at the load circuit.

A. DC Input Voltage and Current

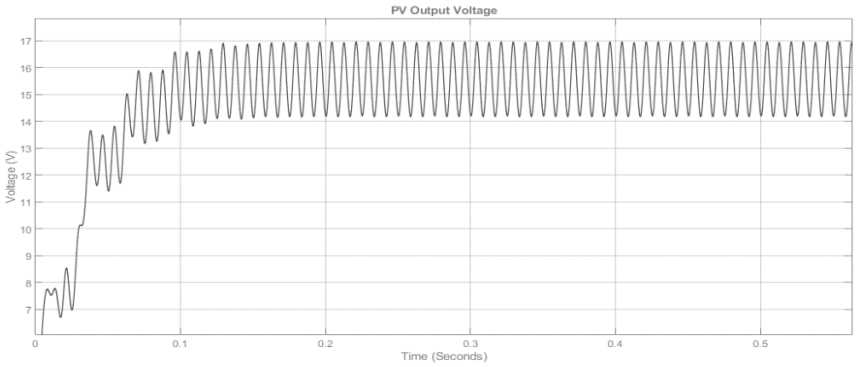

Fig. 7 PV Output Voltage

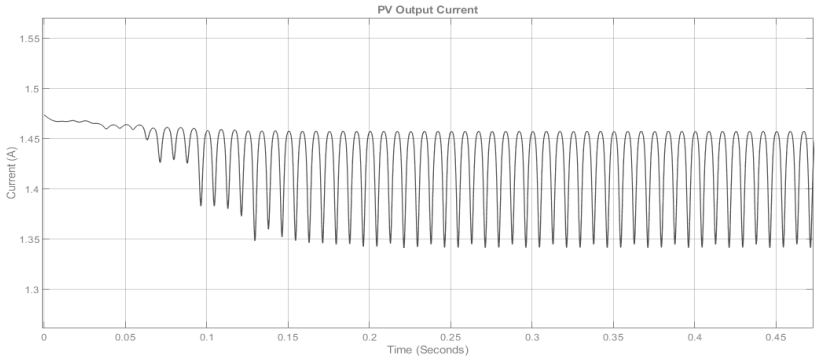

Fig. 8 PV Output Current

The system's configuration includes temperature and radiation as inputs, with voltage and current as outputs. The PV panel processes these inputs to produce PV voltage and current outputs. Fig. 7 and Fig.8 display the simulation outcomes of the PV system operating at 25 degrees temperature and 1000 irradiances. Notably, the results represent the output of the implemented MPPT Algorithm, showcasing its tracking capability. The simulation results indicate a peak voltage of 16.96 volts and 1.47 amperes generated by the PV, which then serves as input to the system.

B. Z Source Network Characteristics

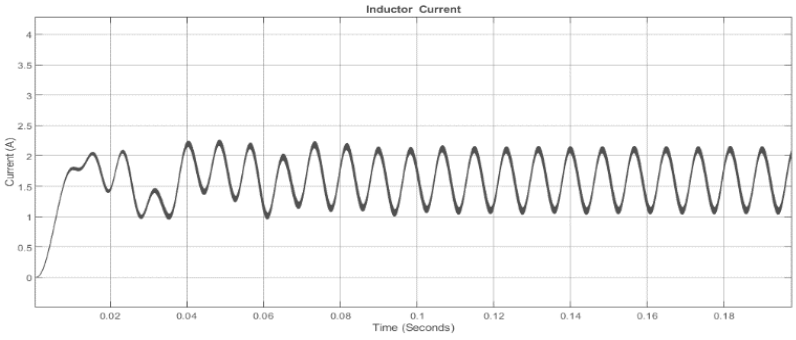

Fig. 9 Z-Source Network Inductor Current

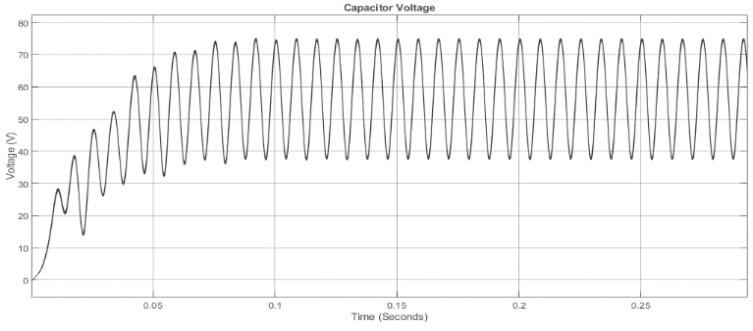

Fig. 10 Z-Source Network Capacitor Voltage

The input signal progresses through the z-source network, which is defined by the interconnection of the crossed Z-shaped components having specific parameters, namely L1=L2=10 mH and C1=C2=47 μF. These precise

component values were derived through rigorous mathematical calculations and subsequently simulated using MATLAB/Simulink. It's worth noting that these component values, particularly the inductance and capacitance, play a crucial role in the system's performance. The inductance value is selected to ensure that the current through it never reaches zero, which is essential for continuous operation. This characteristic is demonstrated in Fig.9, where the current exhibits a smooth waveform without zero-crossings, indicating the appropriate selection of inductance values.

C. AC Output Voltage and Current

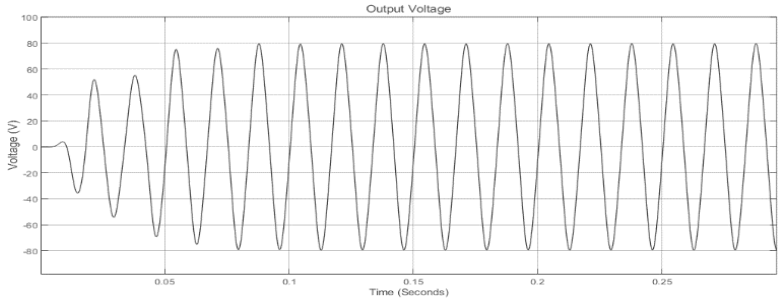

Fig. 11 Output Voltage

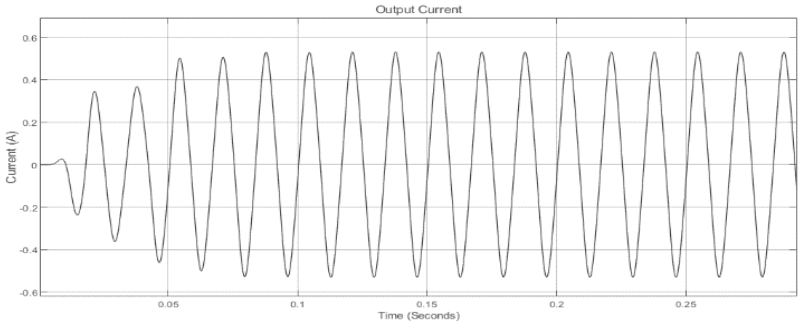

Fig. 12 Output Current

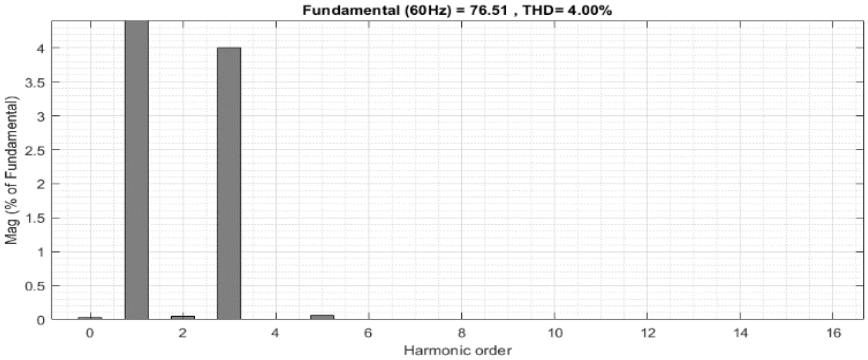

Fig. 13 Fundamental (60Hz) = 0.4545 , THD= 4.03%

Fig.11 and Fig.12 illustrate the inverter's AC output voltage and current obtained from the simulation. Notably, the output voltage reaches a maximum amplitude of 67.81 volts and 0.45 amperes at D=0.49. In the voltage and current waveforms at the output, it is seen that the output unwanted harmonic components are present. As a result of the generation of these components also appear distortion harmonics output voltage and current in the load. As a result, the load voltage and current in the inverter at a frequency of 60Hz contains a THD of 4.03% as seen in Fig.13. This THD is considered low and meets Saudi Arabia's THD approved range [14].

Furthermore, this voltage boosting, enabled by the ZSI, eliminates the need for a boost circuit, reduces components and costs, and facilitates the buck-boost function through one-stage conversion, ensuring a stable high-impedance voltage source with less cost, reliability, and high efficiency.

VI. CONCLUSION

This paper investigates the integration of ZSI design in microinverters for PV systems, aiming to boost voltage output and minimize size. Through MATLAB/Simulink simulations, the system showcases its capability to attain boosted voltage and current outputs from the PV panel, facilitated by MPPT and SBPWM control algorithms. Despite some harmonic distortion, the system meets acceptable standards. Integrating ZSI offers improved efficiency, cost reduction, and stable operation, suggesting promising prospects for renewable energy applications. Further optimization of control mechanisms is recommended for enhanced performance and wider adoption of this technology.

Future work includes implementing ZSI microinverters in grid-tie systems with frequency and phase controllers, along with AI-powered capabilities for autonomous frequency correction, aiming to improve functionality and integration in sustainable energy systems.

REFERENCES

[1] Ali, Amjad, Transforming Saudi Arabia's Energy Landscape towards a Sustainable Future: Progress of Solar Photovoltaic Energy Deployment" Sustainability, vol. 15, 2023, no. 10, 8420, doi: 10.3390/su15108420.

[2] Tlili, I., "Renewable energy in Saudi Arabia: current status and future potentials." Environ Dev Sustain, vol. 17, Sep. 2014, pp. 859–886, doi: 10.1007/s10668-014-9579-9

[3] H. Ribeiro, A. Pinto, and B. Borges, "Single-stage DC-AC converter for photovoltaic systems" 2010 IEEE Energy Conversion Congress and Exposition, Atlanta, GA, USA, 2010, pp. 604-610, doi: 10.1109/ECCE.2010.5617957.

[4] A. S. M. Ranganatha, "Solar Micro Inverter Modeling and Reliability" Arizona State University, 2015, pp. 84-88.

[5] J. Chen, W. Yao, C.-K. Zhang, Y. Ren, and L. Jiang, "Design of robust MPPT controller for grid-connected PMSG-Based wind turbine via perturbation observation based nonlinear adaptive control" Renewable Energy, vol. 134, 2019, pp. 478–495, doi: 10.1016/j.renene.2018.11.048.

[6] N. Singh and S. K. Jain, "Single phase Z-source inverter for photovoltaic system" 2016 7th India International Conference on Power Electronics (IICPE), Patiala, India, 2016, pp. 1-6, doi: 10.1109/IICPE.2016.8079340.

[7] Fang Zheng Peng, "Z-source inverter" in IEEE Transactions on Industry Applications, vol. 39, no. 2, pp. 504-510, March-April 2003, doi: 10.1109/TIA.2003.808920.

[8] Kolantla, D., Mikkili, S., Pendem, S.R. and Desai, A.A, " Critical review on various inverter topologies for pv system architectures " IET Renew. Power Gener, vol. 14, 2020, pp. 3418–3438, doi:10.1049/iet-rpg.2020.0317

[9] D. G, R. Varma, B. V. Ramana, K. Madhu, J. Chandra Shekar and G. Nithin, "Z-source Inverter for Standalone Application" 2023 8th International Conference on Communication and Electronics Systems (ICCES), Coimbatore, India, 2023, pp. 26-31, doi: 10.1109/ICCES57224.2023.10192666.

[10] Y. Huang, M. Shen, F. Z. Peng and J. Wang, " Z -Source Inverter for Residential Photovoltaic Systems" in IEEE Transactions on Power Electronics, vol. 21, no. 6, pp. 1776-1782, Nov. 2006, doi: 10.1109/TPEL.2006.882913.

[11] T. H. Cheng, S. A. Zulkifli and N. M. B. Shah, "Applying of MPPT algorithm in Z source inverter for PV solar generation," 2017 IEEE Conference on Energy Conversion (CENCON), Kuala Lumpur, Malaysia, 2017, pp. 163-168, doi: 10.1109/CENCON.2017.8262477.

[12] S. Kamalakkannan and D. Kirubakaran, " Maximum Power Point Tracking (MPPT) for a PV Powered Z-Source Inverter" Indian Journal of Science and Technology, 2016, vol.9, pp. 1-8, doi:10.17485/ijst/2016/v9i28/95160.

[13] A. Yadav, S. Chandra, V. Deolia and S. Agrawal, "Z source inverter application and control for decentralized photovoltaic system" 2017 3rd International Conference on Condition Assessment Techniques in Electrical Systems (CATCON), Rupnagar, India, 2017, pp. 52-57, doi: 10.1109/CATCON.2017.8280183.

[14] J. C. Das, "Harmonic Distortion Limits According to Standards" in Power System Harmonics and Passive Filter Designs, IEEE, 2015, pp.427-451, doi: 10.1002/9781118887059.